Augmented Reality in Microinvasive Cardiac Surgery: Towards a Training Simulator for Mitral Valve Repair Intervention

Domenico Riggio[1,†], Sofia Breschi[2,†], Angela Peloso[2], Maria Francesca Spadea[1], and Elena De Momi[2]

***Abstract*— Mitral regurgitation is a structural heart condition affecting the mitral valve that can be treated with the MitraClip system™, a device that allows a percutaneous intervention for the deployment of a catheter-embedded clip on the valve leaflets to prevent blood-backflow from the left ventricle to the left atrium. Despite its efficacy, the procedure presents technical challenges, relying on fluoroscopy guidance and surgeon expertise. In the context of human-machine interface for autonomous robotic catheter cardiac intervention, this study aims to evaluate the effectiveness of Augmented Reality (AR) for training surgeons in the MitraClip procedure. Users using an AR Interface demonstrated better performance compared to those using an interface emulating traditional visualization methodologies (fluoroscopy and transesophageal echocardiography). AR-based training offers a more engaging and effective learning experience, leading to improved surgical dexterity and safety in the procedure.**

I. INTRODUCTION

Mitral Regurgitation (MR) is a cardiac condition arising in case of disruption in the mitral valve apparatus, leading to an abnormal blood backflow from the left ventricle to the left atrium, and it can be treated with a structural intervention cardiology procedure. The MitraClip system™ (Abbott™ Illinois, U.S.A.), in Fig.1.A, is a device specifically designed for this procedure, embedded with a catheter called delivery system which enables the delivery of a clip on the leaflets, as shown in Fig.1.B, to avoid blood back-flow into the left atrium [1]. Still, this procedure presents some drawbacks, as it is technically demanding, requires fluoroscopy guidance, hence the use of X-ray radiation, to keep track of the catheter inside the patient, and its outcome relies on the surgeon's skills and experience. The control of this system is complex, and nowadays, surgeons acquire confidence during real patient interventions [2]. The MR intervention with the MitraClip system requires the use of two real-time imaging techniques, such as fluoroscopy and Trans-Esophageal Echocardiography (TEE) [3]. The former, shown in Fig.1.C, is a top planar view used to navigate the delivery system throughout the heart chamber. The latter is used in two different views: the Left Ventricular Outflow Tract (LVOT) view, shown in Fig.1.D, provides an image of the area where the blood flows out of the left ventricle and into the aorta; the commissural, shown in Fig.1.E, provides an image of the mitral valve from the perspective of the valve's commissures. The need to improve surgeons' confidence in structural intervention cardiology procedures arises, leading to an interest in the development of surgical simulators combined with high-level technologies such as Augmented Reality [4]. This study presents the development of an AR Interface to assess the manipulation learning of the MitraClip system, investigating the advantages of an interactive scenario with respect to a 2D screen visualization modality. The ultimate goal is to lay the groundwork for the creation of advanced simulators in the field of mitral valve repair surgery in order to give surgeons an advanced tool for practicing the procedure and increasing their dexterity with the system in a simulated environment.

II. STATE OF THE ART

AR in surgery and surgical training

The fundamental learning elements across surgical specialties are still based on observation, practical experience, and an in-depth understanding of three-dimensional anatomical arrangements [5]. Traditionally, cadaveric models and expert guidance have represented the cornerstone of medical and surgical education. However, over the last decade, the advent of surgical simulations and AR tools has aimed to improve practical surgery training [6]. In this sense, AR leads to a multitude of advantages providing for example access to real-time, patient-specific 3D anatomical images and models. Moreover, AR may enhance preoperative planning improving surgical outcomes by offering intraoperative guidance [7] or reducing preparation times, establishing low-risk environments for surgical testing, and limiting personnel and surgical equipment-related costs [7]. In such a scenario, the application of AR extends already across various surgical disciplines, with notable prevalence in the United States, Germany, China, and Canada where AR is implied for medical students, residents, and surgeons' training and education, particularly in orthopedics and neurosurgery, for example for brain oncology and spinal surgery [8], gaining more and more popularity considering its high versatility [9][10][11]. In the context of neurosurgery for example, AR exhibits significant advantages, allowing for efficient processing times and the practice of major neurosurgical procedures outside the operating room, thereby establishing a practical training framework in a protected environment [12]. Current literature supports the positive impact of AR on surgical training, consistently reducing learning curves and bridging the expertise gap between novice students and experienced practitioners [13][14][15]. In this sense, competency and surgical opinion resulted higher in the case of AR use [16]. Considering these enthusiastic data, our project

[†]These authors contributed equally to this work.

*This work was funded by the European Union - Next Generation EU.

[1]Faculty of Electrical Engineering and Information Technology, at the Institute of Biomedical Engineering, Karlsruhe Institute of Technology, Germany. domenico.riggio@kit.edu, publications@ibt.kit.edu

[2]Department of Electronics, Information and Bioengineering, Politecnico di Milano, Italy. sofia.breschi@polimi.it

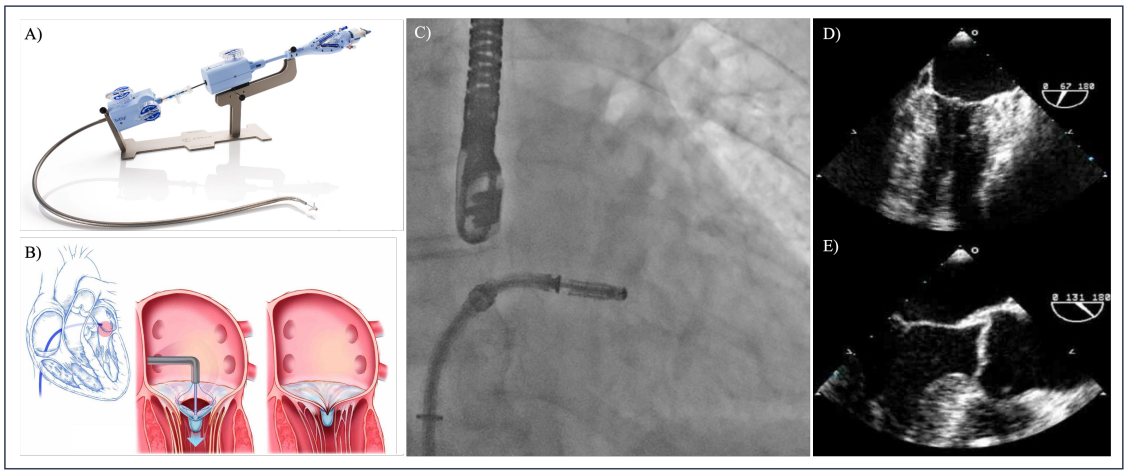

Fig. 1. Standard Procedure. A) The MitraClip system™ (Abbott™ Illinois, U.S.A.); B) Mitraclip procedure scheme: clip grasping leaflets; C) Intraoperative fluoroscopy image [17]; D) Intraoperative Commisural image [17]; E) Intraoperative LVOT image [17].

aims to investigate the AR's potential positive contributions to the learning process of technically demanding surgeries such as the MitraClip procedure.

III. Materials and Methods

Our system, displayed in Fig. 2.A, consisted of: a cardiovascular anatomical phantom, the phantom support base, the MitraClip system, and the Electromagnetic sensor (EM) (Aurora™ NDI, Waterloo, Canada) for the calibration procedure. The silicon vein phantom was obtained from a computed tomography scan of a MitraClip candidate provided by IRCCS Ospedale San Raffaele, Milan, Italy. The phantom base was 3D-printed in order to support and stabilize the vein phantom and the MitraClip inside of it. Furthermore, it was designed with six columns to allow the calibration with the simulator. The MitraClip was inserted into the phantom to emulate the surgical scenario.

Simulation Environment

The Simulation Environment (SE) was built in Unity3D [18], with the 3D models of the mitral valve, the left heart chambers, the vein, the phantom base, and the MitraClip system replicating the physical setup, as illustrated in Fig. 2.B. Starting from the SE, two interfaces were built. The first simulates the state-of-the-art for image guided navigation proposed in Fig. 1.C, and the latter presents the AR experience, respectively called 2D Interface and AR Interface.

2D Interface: The 2D Interface was built with three fixed views, emulating the style of fluoroscopy guidance and the two TEE views: the Commissural view and the LVOT. The first view was obtained by under-imposing the navigation scene onto a grey-scale image, with no specific anatomical reference as it is available in real practice. The latter views were obtained by sectioning the heart model with two different planes: one accounting for the Commissural cut and the other for the LVOT. Therefore, the user is presented with a section of the heart cavities on a black background. This display provides anatomical references for the atrium, ventricle, and mitral valve. The view that mimics the style of fluoroscopy allows the user to visualize the navigation scene throughout the entire procedure. On the other hand, the views simulating TEE visualizations give the user the possibility to visualize the catheter only in proximity to the valve when positioned correctly to reach the target point.

AR Interface: The AR Interface was developed to leverage augmented reality features, including manipulation of holograms, scaling, and color adjustments, utilizing a head-mounted display. This interface, illustrated in Fig. 2.D, offers users a 3D view of the experimental setup, enhancing spatial perception and enabling them to adjust holograms to suit their preferences.

Catheter Modeling

The delivery system is a tendon-driven catheter whose control is allowed through the presence of knobs (illustrated in Fig. 1.A). Through the rotation of the knobs, it is possible to pull or release the inner tendons of the catheter, allowing to manage the bending in the Medio-Lateral (ML) and Anterior-Posterior (AP) plane. The system is actuated by three tendons, two of them for the AP movement and one for the ML movement. Although the MitraClip delivery system has only three cables, these are shifted 90 degrees to one another and have the typical four tendon configuration. The Constant Curvature (CC) method was chosen in order to model the catheter kinematic and to represent it in the SE. The CC model characterizes the continuum robot geometry with a finite number of mutually tangent curved segments each having a constant curvature along its length. Each segment is described by its *arc parameters* curvature κ, length ℓ, and angle ϕ that completely define the shape of the backbone. To retrieve the catheter shape from the EM signal, which corresponds to the tip position, it was necessary to build an inverse kinematic (IK) model, displayed in Fig. 3. Using as input the pose of the

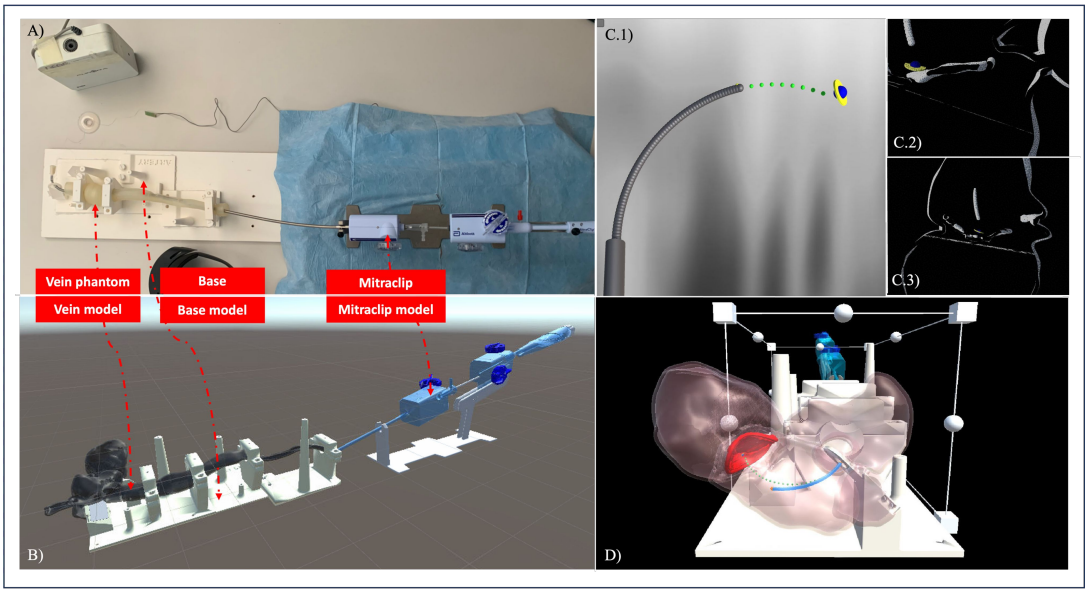

Fig. 2. Our approach. A) Physical setup; B) SE; C) 2D Interface: C.1) Fluoroscopy simulation, C.2) LVOT simulation, C.3) Commissural simulation; D) AR Interface. In C) and D) the green dotted line represents the best trajectory.

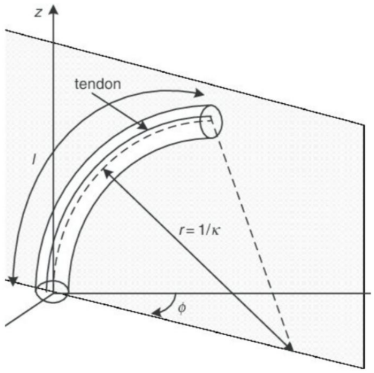

Fig. 3. Constant Curvature arc with length l, bending with curvature k in the plane identified by the angle ϕ [19].

EM, it is possible to compute the arc parameters κ, ℓ, and ϕ with the following equations [19]:

$$\phi = \tan^{-1}\left(\frac{y}{x}\right) \tag{1}$$

$$k = \frac{2\sqrt{x^2 + y^2}}{x^2 + y^2 + z^2} \tag{2}$$

$$l = \frac{\cos^{-1}(1 - k\sqrt{x^2 + y^2})}{k} \tag{3}$$

Once the values of κ, ℓ, and ϕ have been calculated, it was possible to map them to the length of the cables by means of the following geometrical relationship:

$$q_i = -r\theta \cos\left(\left(\frac{\pi}{2}\right) i - \phi\right) \quad i = 0, 1, 2 \tag{4}$$

where $\theta = \kappa\ell$ and r is the distance between the i^{th} cable and the central backbone in the cross-sectional plane. In this way the mapping between the length of each cable and the desired pose is completed, allowing the building of the shape of the catheter with respect to the pose updated by the sensor signal. The reconstruction of the catheter shape can be observed in the simulator's interfaces in the light grey dotted line in Fig. 2.C.1, in the light grey dotten line in Fig. 2.C.2,2.C.3 and light blue in Fig. 2.D respectively.

Calibration and Communication protocol

To establish precise calibration between the patient system, i.e. the physical setup, and the SE, an EM sensor was employed, and the singular value decomposition technique was chosen to pair the two systems. This technique involves collecting a set of points in the physical setup system and the corresponding set of points in the simulation environment [20]. The calibration scheme is illustrated in Fig. 4. Once the transformation matrix T_{EM}^{SE} was computed, a sensor could be attached to the distal part of the delivery system to track its movements in the SE. The transformation matrix T_{SE}^{AR} to pair the SE and the AR environment is automatically computed by the AR head-mounted device.
Robotic Operative System (ROS) [21] allowed communication between the EM, SE, and the AR head-mounted device. Due to the high computational cost of IK, it was necessary to compute it in the SE, using the AR head-mounted device solely for visualization. As shown in the scheme in Fig. 4, channels 1 and 2 are used to communicate the tip pose to the SE. The SE computes the IK and uses channels 3 and 4 to communicate the data about the catheter shape to the AR head-mounted device. The Calibration Error (CE) was computed as the mean value of the Euclidean distance between a set of six fixed points in the simulated environment and the corresponding six position values of the EM. The calibration system used was proved to be efficient, registering a CE of 2.92 ± 0.31 mm over 10 acquisitions by the same

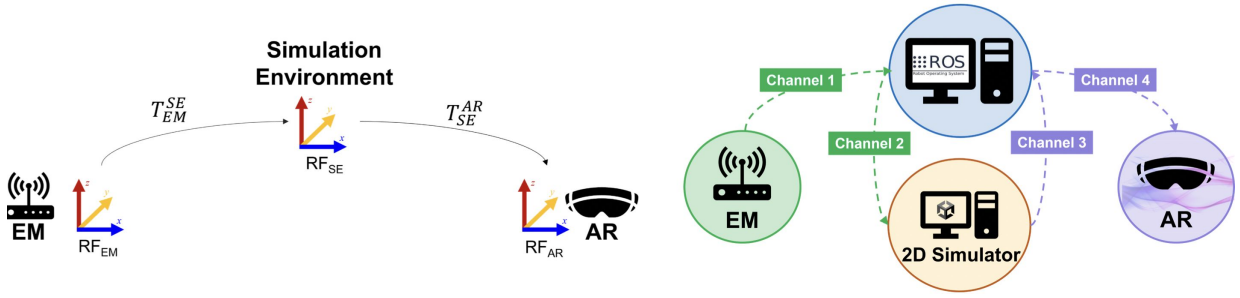

Fig. 4. Calibration scheme on the left, and communication protocol on the right.

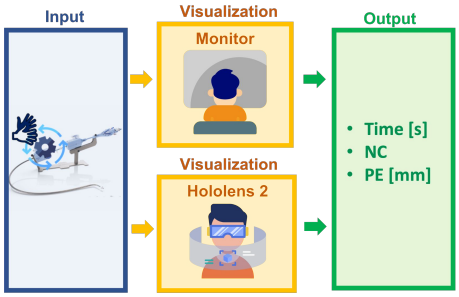

Fig. 5. Task protocol. Input: Hands maneuvering of the knobs; Visualization: 2D/AR Interface; Output: collected parameters.

operator, thus providing a good pairing between the physical system and the SE.

IV. Experiments

Setup

The experimental configuration presented in Fig. 2.A included a vascular anatomical phantom, its support base, the MitraClip system, and an EM sensor (Aurora™ NDI, Waterloo, Canada). The user was introduced to one of the two implemented interfaces as a visualization system, concealing the distal part of the physical catheter and its movements during the experiments. The 2D Interface was provided through a standard monitor while the AR Interface was provided through a head-mounted device, in particularly for this study Hololens 2™ (Microsoft™ Redmond, U.S.A.) [22] was chosen.

Protocol

The participants were asked to manipulate the physical MitraClip system, controlling the knobs while watching the simulation with the real-time catheter reconstruction using one of the two proposed visualization modalities. Throughout the experiments, performance metrics were gathered and later a questionnaire was administrated. The protocol is schematized in Fig. 5. 24 participants were recruited and asked to perform the task with the visualization system assigned to their group. The age of the participants has a median of 25 and a variance of 3.44, and they all have a bioengineering background. Among the 24 subjects, only 7 did not have prior experience with AR/VR. All the users provided informed consent before participating, and the experimental protocol was approved by the ethics committee of Politecnico di Milano, Italy (No. 45/2023).

Task

To avoid any bias due to learning, users were randomly divided into two groups according to the assigned visualization system. Every participant was asked to navigate the digital twin of the catheter, following the optimal trajectory (i.e. green dotted line), to the target (yellow and blue object) without colliding with the heart chambers. When the target was successfully reached, the user would perform the next trial for a total of 5 consecutive trials.

Evaluation Metrics

During the experiments, the following evaluation metrics were recorded:

(1) Time [s] was computed as the difference between the start of the trial T_0 and the end of the trial T_f.

$$Time = T_f - T_0 \tag{5}$$

(2) The number of collisions (NC) was determined for each trial by summing the collisions that occurred between the tip of the digital catheter and the heart's walls.

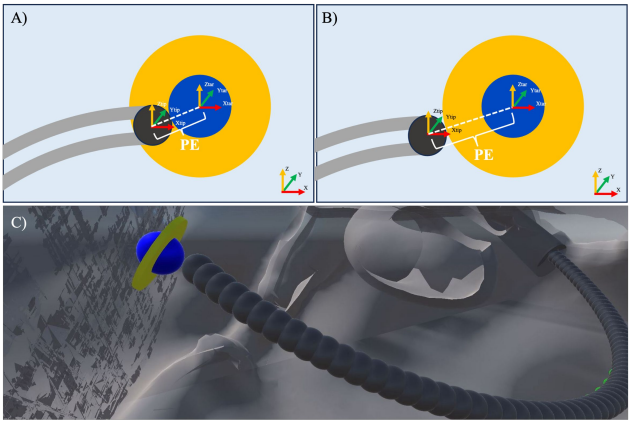

Fig. 6. PE is measured as the Euclidean distance d between the center of the sphere composing the tip of the catheter model and the target object. In A) is represented the PE when the catheter's tip hits the blue part of the target, in B) the PE when the yellow part of the target is hit, and in C) is displayed the collision between the tip of the catheter and the target in the SE.

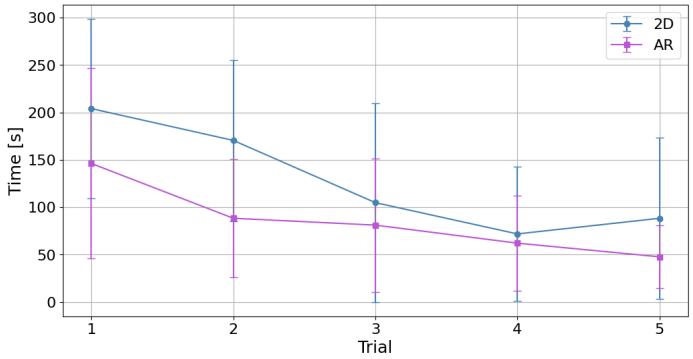

Fig. 7. Learning curves depicting time performance, with median values and interquartile ranges, for the 2D Interface (in blue) and the AR Interface (in purple).

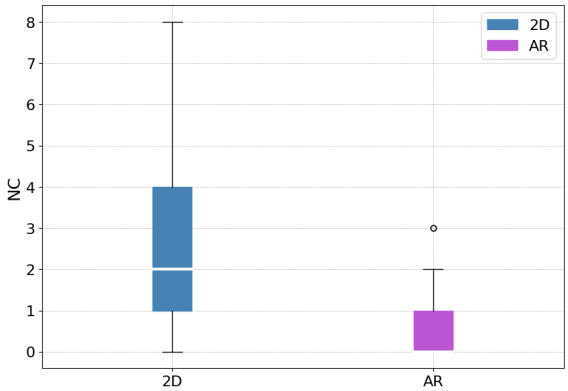

Fig. 8. NC boxplots. Data distribution of the NC of all the repetitions of all the users recorded with the 2D Interface and AR Interface.

(3) The position error (PE) [mm], shown in Fig. 6 was computed by measuring the Euclidean distance between the catheter tip position $_{tip}$ and the target position $_{tar}$ as follows:

$$PE = \sqrt{(x_{tip} - x_{tar})^2 + (y_{tip} - y_{tar})^2 + (z_{tip} - z_{tar})^2} \quad (6)$$

Due to the physical meaning of the objects in Unity3D, the final PE data was retrieved by subtracting to the recorded values the thickness of the target mesh as well as the radius of the catheter's tip sphere mesh.

(4) At the end of the experiments, to evaluate the user's experience, participants were asked to complete the NASA Task Load Index (NASA-TLX), a standardized questionnaire designed to assess perceived workload during an activity.

V. Results and Discussions

The results obtained from the user study, when subjected to the Shapiro-Wilk Test, exhibited a non-normal distribution. For Time, NC, and PE results the Mann-Whitney U test was performed for the two populations, reporting Time p_value = $1.94x10^{-3}$, NC p_value = $3,725x10^{-8}$ and PE p_value = $2.9x10^{-5}$, highlighting their statistical difference. Time results are presented through learning curves in Fig. 7, NC and PE results are shown with boxplots respectively in Fig. 8 and 9, and the subjective user's evaluations are reported through

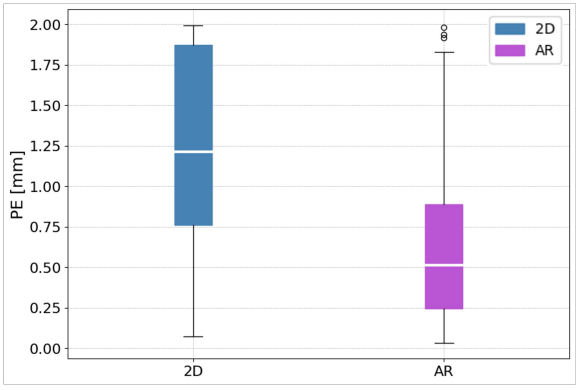

Fig. 9. PE boxplots. Comparative analysis of the PE of all the repetitions of all the subjects recorded with the 2D Interface and AR Interface.

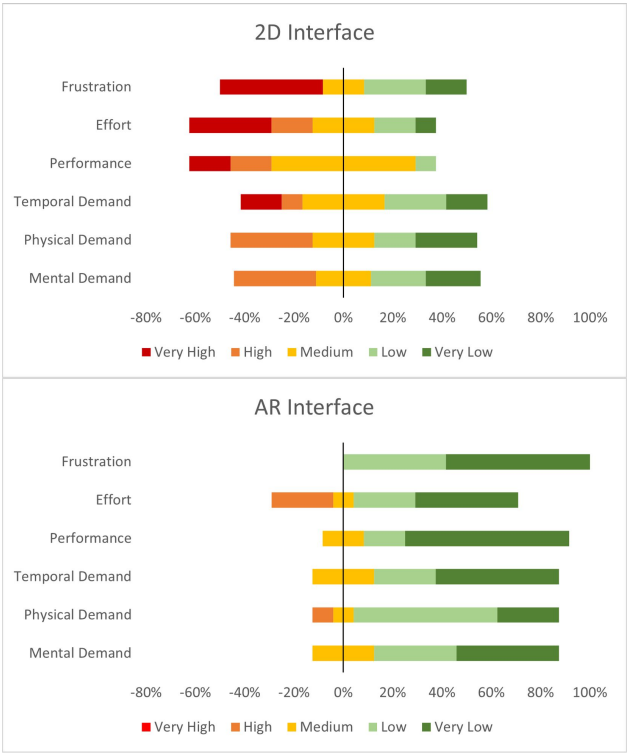

Fig. 10. Likert chart of the NASA-TLX questionnaires for the 2D and AR Interfaces, with lower scores indicative of better evaluation on the utilised scale.

Likert charts in Fig. 10. Regarding the learning curves, the median values for every trial are retrieved considering the performances of all the participants. This study revealed that better results were obtained across all metrics in the visualization modality that leverages AR. More specifically, observing the learning curve in Fig. 7, the median Time in seconds of the AR Interface group per each trial is lower than the one recorded for the 2D Interface group. Moreover, for the AR Interface group the values decrease from the first to the last trial, on the contrary, the same trend is not visible for the 2D Interface group, which provides worse Time results along the curve especially on the last trial. The NC is presented through the boxplots in Fig. 8. It emerges that in the AR

Interface, having the user awareness of the 3D space, the inadvertent contacts with the heart walls were significantly lower than the ones registered using the 2D Interface, hence highlighting the possible improvement in the procedure's safety. Regarding the PE, the boxplots in Fig. 9 show that even if the users were all able to reach the target position, the group using the AR Interface was more successful in reaching the center of the target, therefore being able to follow the proposed trajectory. In addition, the results obtained using AR in all evaluated metrics show less variance, indicating more predictability and stability.

The subjective assessment is reported in Fig. 10. The Likert charts display that the score's distribution for the AR Interface is shifted toward the lowest values, reporting just a few negative evaluations. It highlights that users perceived improved performance, decreased effort, and reduced frustration when using the AR Interface with respect to the 2D Interface. Furthermore, the low mental and physical demands indicate that the system is relatively intuitive and user-friendly.

VI. CONCLUSIONS

In this work, an AR training simulator for mitral valve repair procedures was developed. Our study highlights the potential of this innovative technology, showcasing advantages in terms of patient safety. The overall analyses suggest that the AR Interface offers a more engaging and effective learning experience, reduced learning time, minimized occurrences of collisions, and a lower PE with respect to the 2D Interface. Users reported a more favorable experience, reflecting positively on performance, mental effort, and overall satisfaction with the system. This subjective assessment aligns with the objective metrics, reinforcing the conclusion that the AR Interface stands out as an effective and user-friendly training tool. It is important to acknowledge a limitation of our study, specifically about the echography simulation within the 2D Interface. Recognizing its potential for improvement, future works should focus on refining this aspect to offer a more faithful representation of the real surgical scenario. Further developments could also include developing deformable models for heart and catheter and integrating realistic heartbeat and respiration motion. These advancements would improve the simulator's realism, thereby providing an even more immersive and comprehensive training environment for mitral valve repair procedures.

References

[1] Perlowski A, Feldman T. Percutaneous Treatment of Mitral Regurgitation: The MitraClip Experience. Interv cardiol Clin. 2012 Jan;1(1):63-72. doi: 10.1016/j.iccl.2011.09.007. Epub 2012 Feb 9. PMID: 28582068.

[2] Chhatriwalla AK, Vemulapalli S, Holmes DR Jr, Dai D, Li Z, Ailawadi G, Glower D, Kar S, Mack MJ, Rymer J, Kosinski AS, Sorajja P. Institutional Experience With Transcatheter Mitral Valve Repair and Clinical Outcomes: Insights From the TVT Registry. JACC cardiovasc Interv. 2019 Jul 22;12(14):1342-1352. doi: 10.1016/j.jcin.2019.02.039. PMID: 31320029.

[3] Sherif MA, Paranskaya L, Yuecel S, Kische S, Thiele O, D'Ancona G, Neuhausen-Abramkina A, Ortak J, Ince H, Öner A. MitraClip step by step; how to simplify the procedure. Neth Heart J. 2017 Feb;25(2):125-130. doi: 10.1007/s12471-016-0930-7. PMID: 27933588; PMCID: PMC5260622.

[4] Lungu AJ, Swinkels W, Claesen L, Tu P, Egger J, Chen X. A review on the applications of virtual reality, augmented reality and mixed reality in surgical simulation: an extension to different kinds of surgery. Expert Rev Med Devices. 2021 Jan;18(1):47-62. doi: 10.1080/17434440.2021.1860750. Epub 2020 Dec 16. PMID: 33283563.

[5] Cannizzaro D, Rammos SK, Peschillo S, El-Nashar AM, Grande AW, Lanzino G. The lateral mesencephalic vein: surgical anatomy and its role in the drainage of tentorial dural arteriovenous fistulae. World Neurosurg. (2016) 85:163–8. doi: 10.1016/j.wneu.2015.08.060

[6] Yoon JW, Chen RE, Kim EJ, Akinduro OO, Kerezoudis P, Han PK, et al. Augmented reality for the surgeon: systematic review. Int J Med Robot.(2018) 14:e1914. doi: 10.1002/rcs.1914

[7] https://builtin.com/healthcare-technology/augmented-virtual-reality-surgery

[8] Cannizzaro Delia, Zaed Ismail, Safa Adrian, Jelmoni Alice J. M., Composto Antonio, Bisoglio Andrea, Schmeizer Kyra, Becker Ana C., Pizzi Andrea, Cardia Andrea, Servadei Franco. Augmented Reality in Neurosurgery, State of Art and Future Projections. A Systematic Review. Frontiers in Surgery. (2022) 10.3389/fsurg.2022.864792

[9] Tagaytayan R, Kelemen A, Sik-Lanyi C. Augmented reality in neurosurgery. Arch Med Sci. (2018) 14:572–8. doi: 10.5114/aoms.2016.58690

[10] Guha D, Alotaibi N, Nguyen N, Gupta S, McFaul C, Yang V. Augmented reality in neurosurgery: a review of current concepts and emerging applications. Can J Neurol Sci. (2017) 44:235–45. doi: 10.1017/cjn.2016.443

[11] Zhu E, Hadadgar A, Masiello I, Zary N. Augmented reality in healthcare education: an integrative review. PeerJ. (2014) 2:e469. doi: 10.7717/peerj.469

[12] Meola A, Cutolo F, Carbone M, Cagnazzo F, Ferrari M, Ferrari V. Augmented reality in neurosurgery: a systematic review. Neurosurg Rev. (2017) 40:537–48. doi: 10.1007/s10143-016-0732-9

[13] Cofano F, Di Perna G, Bozzaro M, Longo A, Marengo N, Zenga F, et al. Augmented reality in medical practice: from spine surgery to remote assistance. Front Surg. (2021) 8:657901. doi: 10.3389/fsurg.2021.657901

[14] McKnight RR, Pean CA, Buck JS, Hwang JS, Hsu JR, Pierrie SN. Virtual reality and augmented reality-translating surgical training into surgical technique. Curr Rev Musculoskelet Med. (2020) 13:663–74. doi: 10.1007/s12178-020-09667-3

[15] Zaed I. COVID-19 consequences on medical students interested in neurosurgery: an Italian perspective. Br J Neurosurg. (2020) 6:1–2. doi: 10.1080/02688697.2020.1777260

[16] Matthew Adam Williams, James McVeigh, Ashok Inderraj Handa, Regent Lee, Augmented reality in surgical training: a systematic review, Postgraduate Medical Journal, Volume 96, Issue 1139, September 2020, Pages 537–542, https://doi.org/10.1136/postgradmedj-2020-137600

[17] "MR Procedure": https://www.youtube.com/watch?v=OTSZ1m3uqDE.

[18] "Unity Engine": https://unity.com.

[19] Webster RJ, Jones BA. Design and Kinematic Modeling of Constant Curvature Continuum Robots: A Review. The International Journal of Robotics Research. 2010;29(13):1661-1683. doi:10.1177/0278364910368147.

[20] M. C. Palumbo et al., "An Easy and User Independent Augmented Reality Based Navigation System for Radiation-Free Interventional Procedure," 2022 International Symposium on Medical Robotics (ISMR), GA, USA, 2022, pp. 1-7, doi: 10.1109/ISMR48347.2022.9807461.

[21] "Robotic Operating System (ROS)": https://www.ros.org.

[22] Palumbo, A. Microsoft HoloLens 2 in Medical and Healthcare Context: State of the Art and Future Prospects. Sensors 2022, 22, 7709. https://doi.org/10.3390/s22207709.